High Resolution Atomic Coherent Control via Spectral Phase Manipulation of an Optical Frequency Comb

Matthew C. Stowe, Flavio C. Cruz,* Adela Marian,† and Jun Ye

JILA, National Institute of Standards and Technology and University of Colorado, Department of Physics, University of Colorado, Boulder, Colorado 80309-0440, USA
(Received 8 February 2006; published 17 April 2006)

We demonstrate high resolution coherent control of cold atomic rubidium utilizing spectral phase manipulation of a femtosecond optical frequency comb. Transient coherent accumulation is directly manifested by the enhancement of signal amplitude and spectral resolution via the pulse number. The combination of frequency comb technology and spectral phase manipulation enables coherent control techniques to enter a new regime with natural linewidth resolution.

The introduction of phase-stabilized optical frequency combs has revolutionized the field of precision atomic and molecular spectroscopy [1,2]. In our previous work we used direct frequency comb spectroscopy (DFCS) to demonstrate high resolution measurements of one- and two-photon transitions in cold ^{87}Rb [3,4]. This new technique has the significant advantage that the comb frequencies may be absolutely referenced to a cesium atomic clock, enabling precision spectroscopy over a bandwidth of several tens of nanometers. The time-domain phase coherence offered by the optical frequency comb has stimulated research in areas of atomic clocks [5,6], optical and radio frequency transfer [7], and more recently high harmonic generation [8,9]. In parallel, the field of coherent control of atomic and molecular systems has seen advances incorporating high power femtosecond laser sources and pulse shaping technology. This has allowed demonstrations of robust population transfer via adiabatic passage techniques [10,11], coherent control of two-photon absorption [12–14], resolution enhancement of coherent anti-Stokes Raman scattering [15], and research on cold atom photoassociation [16]. It is under this exciting context that we combine the femtosecond comb and spectral phase manipulation with the aim towards coherent control at the highest possible resolution.

In this Letter, properties of the transient coherent accumulation effect, including spectral phase manipulation, are explicitly demonstrated via a finite number of phase-stabilized femtosecond pulses. Specifically, we measure atomic transition linewidth and population transfer versus the number of applied phase-coherent femtosecond pulses and as a function of linear frequency chirp. The basic idea of multipulse coherent accumulation is that the transition amplitude for excitation of a specific atomic energy level may be increased significantly with the number of femtosecond pulses, while other nonresonant states remain unexcited, thus enabling high state selectivity. We show that tuning the comb leads to destructive quantum interference of the two-photon transition amplitude only observable in this multipulse context and may be useful for eliminating

nonlinear absorption. Positive or negative linear frequency chirp is then applied to the comb modes and thus the two-photon transition amplitudes. It is shown that the role of chirp in the single-pulse case is no longer necessarily applicable in these multipulse experiments since the atomic coherence persists between femtosecond pulses. The combination of pulse shaping with the femtosecond comb is shown to increase the signal of a two-photon transition at a specific chirp while maintaining high resolution.

The spectrum of a train of femtosecond pulses is a set of approximately 10^6 comb modes equally spaced by the repetition frequency (f_r) of the mode-locked laser. The frequency of each comb mode is given by the relation $\nu_N = f_o + N \times f_r$, where f_o is the carrier-envelope offset frequency and N is an integer mode number of the order 10^6 [2]. The frequencies of the comb modes are independent of the spectral phase provided all pulses in the train have the same spectral phase. For the two-photon transitions we investigate, there are of the order $2N$ different transition amplitudes from the ground to the excited state. It is instructive to consider the frequency spectrum of the laser field consisting of a finite number of pulses. In this work we use from 1 to 140 pulses for atomic excitation. The linewidth of the laser field after a single pulse is approximately 30 nm, and after two pulses the spectrum is sinusoidally modulated at f_r. In general, a comb mode line shape is described by a sinc^2 function of the pulse number. As the linewidth narrows, the power of any comb mode grows as the number of pulses squared. This amplitude and spectral resolution enhancement presents a clear distinction from previous single-pulse excitation experiments.

To explore the transient coherent accumulation effects, we excite a sample of ^{87}Rb atoms in a magneto-optic trap (MOT). This allows for approximately 50 pulses to coherently interact with the atomic system via the $5S_{1/2}$ $F = 2$ to $5P_{3/2}$ $F = 3$ to $5D_{5/2}$ $F = 4$ two-photon transition [Fig. 1(a)]. We use a Kerr lens mode-locked Ti:sapphire laser which operates at a center wavelength of 778 nm with

a 30 nm wide spectrum and 100 MHz repetition rate. This produces transform-limited pulses of approximately 40 fs duration. f_o is measured via the typical f-$2f$ interferometer technique and locked to a stable radio frequency (rf) source which is fixed at a prescribed value or scanned. f_r is stabilized via a Cs-referenced low phase-noise rf source and steered so as to maintain the appropriate absolute frequency of the comb modes. In the following experiments, f_r is locked to 100.413 567 30 MHz, which for f_o values of either 18.14 MHz or -31.86 MHz ensures two-photon resonance between the $5S_{1/2}$ $F = 2$ ground state and $5D_{5/2}$ $F = 4$. For $f_o = 18.14$ MHz, there is a comb mode resonant with the intermediate state $5P_{3/2}$ $F = 3$. In the other case of $f_o = -31.86$ MHz, no mode is resonant with $5P_{3/2}$ $F = 3$, but rather all modes are symmetrically detuned around this intermediate resonance. The signal is proportional to the 5D population and is measured by photon counting the 420 nm $5D$-$6P$-$5S$ cascade fluorescence. For the chosen values of f_r and f_o, the signal after a sufficient number of pulses to reach steady-state excitation is only from the $5D_{5/2}$ $F = 4$ hyperfine level [3]. After many pulses all other 5D and 7S hyperfine states, although covered by the 30 nm comb spectrum, are detuned many linewidths away from the closest comb modes and as a result remain unexcited.

The theory model describing the experimental results is based on numerical solution of the Liouville equation for the density matrix of the three-level atomic system. Decoherence of the electronic system is included via phenomenological decay terms due to the natural linewidth of 6 MHz for the 5P and 660 kHz for the 5D atomic states. The driving field is taken to be a linearly chirped pulse of 30 nm bandwidth at 778 nm and a transform limited peak field strength of $E_o = 10^7$ V/m. After numerically solving for a single pulse, the density matrix is advanced in time to the next pulse analytically, then repeated for an arbitrary number of pulses. This technique differs from some previous work on modeling two-photon coherent control with femtosecond pulses as it is nonperturbative, includes effects of atomic decoherence, and the impulsive excitation approximation is not used [14,17]. Our model includes only the $5S_{1/2}$ $F = 2, 5P_{3/2}$ $F = 3, 5D_{5/2}$ $F = 4$ hyperfine levels. Because the comb is tuned on resonance with this transition, the three-level model is a good approximation to our experiment after several pulses. However, for excitation by few pulses the other hyperfine states cannot necessarily be considered off resonance because the frequency comb structure of the field is not manifest.

The data acquisition cycle [Fig. 1(b)] consists of loading the MOT, shutting off all MOT-related fields, then exciting the free cold atoms. A Pockels cell with 8 ns rise time is used as a fast shutter to transmit any desired number of pulses to the atoms. The triggering for the Pockels cell is derived directly from the laser repetition frequency to ensure that the Pockels cell is always fully on or off
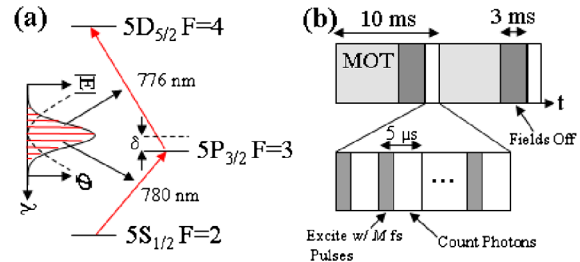

FIG. 1 (color online). (a) Simplified energy level diagram of the three relevant atomic states and frequency domain representation of the chirped comb. δ is the detuning of the intermediate state from half the two-photon transition frequency. (b) Timing diagram used in the experiments.

when a femtosecond pulse is incident. Tunable linear frequency chirp is generated by a double pass grating stretcher and compressor [18], which allows for chirp up to $\phi'' = \pm 2.5 \times 10^5$ fs^2, defined as $\phi'' = d^2\phi/d\omega^2$. Some higher order dispersion is present, but our data are generally well modeled by the inclusion of only quadratic spectral phase. The MOT is loaded for 6 ms, then the magnetic field is turned off for 3 ms during which time an optical molasses remains; finally the atoms are probed after all other fields are off. The timing diagram in [Fig. 1(b)] shows the atoms are excited by M pulses, spontaneously emitted photons are counted for 5 μs, then repeated 40 times per MOT.

We first demonstrate the coherent accumulation of a controlled number of femtosecond pulses on the $5D_{5/2}$ $F = 4$ population and line shape. Previous work on DFCS [3,4] was conducted only under steady-state atomic excitation, i.e., excitation times longer than the atomic coherence time. We investigate properties of the transient femtosecond coherent accumulation for pulse numbers, or equivalently excitation times significantly less than the 240 ns $5D_{5/2}$ $F = 4$ atomic lifetime. The f_r and f_o of the comb are tuned to 100.413 567 30 MHz and 18.14 MHz, respectively (Fig. 2 inset). We split the probe laser and counterpropagate the two intensity-matched beams through the atoms to balance the radiation pressure and thus minimize any line broadening due to accumulated recoil shifts. For the chirped excitation experiments described later, the laser is not counterpropagated. The femtosecond probe laser is focused with linear polarization to a diameter of 160 μm into the MOT, resulting in an electric field strength per beam of approximately 10^7 V/m. Figure 2 shows the total number of photon counts (in squares) that occur after the Mth pulse and is a measure proportional to the total 5D population after excitation by M pulses. The dashed line in Fig. 2 is the result from our theory model for low power multipulse excitation such that there is no power broadening of the linewidth. In the actual experiment the pulse intensity is high enough to excite a significant 5D population and it saturates to its maximum value at a smaller number of pulses than in the case of weak
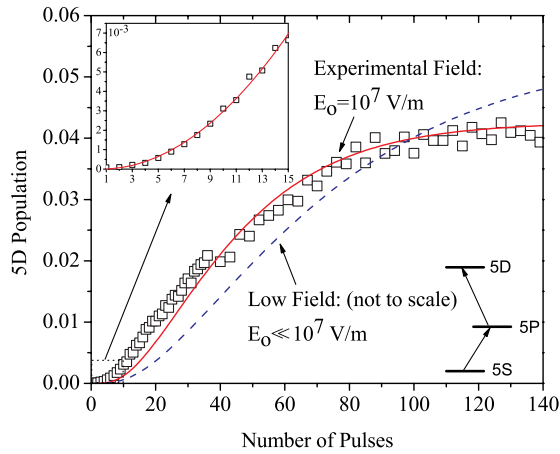
FIG. 2 (color online).   The on-resonance $5D_{5/2}$ $F = 4$ fluorescence signal is measured (squares) at a field strength of $E_o = 10^7$ V/m vs the number of pulses. The solid (dashed) line is the theoretically predicted excited state populations under experimental (asymptotically low) field strengths. The inset shows the quadratic scaling for the first 15 pulses.
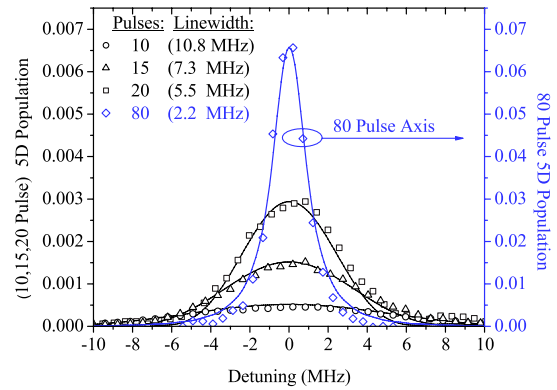

FIG. 3 (color online).   The $5D_{5/2}$ $F = 4$ line shape is measured (symbols) vs the number of applied femtosecond pulses (10, 15, 20, 80 pulses) with the corresponding FWHM linewidth in the legend. The Lorentzian linewidth of 2.2 MHz after 80 pulses is the asymptotic power-broadened linewidth.

excitation (Fig. 2). This is the time-domain picture of power broadening of the transition linewidth due to the femtosecond probe laser. For pulse numbers significantly smaller than the $5D$ coherence time the population scaling can be fit well by a second order polynomial in the pulse number or equivalently the accumulated pulse area (inset Fig. 2). This coherent enhancement of the population versus pulse number demonstrates the increased efficiency over excitation by a single pulse of the same total power for two-photon absorption via a resonant intermediate state.

The coherent accumulation that enables the large enhancement of the resonant $5D$ population simultaneously enables the high resolution necessary for exciting a single $5D$ hyperfine level. In this part of the experiment the line shape is measured by scanning f_o after excitation from M pulses to directly demonstrate the resolution enhancement. The spectral content of the field generated by a finite number of pulses is a series of modes each with a linewidth inversely proportional to the number of pulses coherently accumulated. Figure 3 illustrates this effect through the line shape and width of the measured $5D_{5/2}$ $F = 4$ resonance after excitation by 10, 15, 20, and 80 pulses. The asymptotic power-broadened linewidth of 2.2 MHz occurs at 80 pulses which is approximately the number of pulses for the $5D_{5/2}$ $F = 4$ population in Fig. 2 to saturate.

Some of the original work on coherent control has demonstrated the modification of the quantum interference of two-photon transition in Rb, Cs, and Na by shaping a single femtosecond pulse [12–14]. It was shown that for the transition from $5S$ to $5D$ in Rb the excited state population was essentially zero for large negative chirp, where higher frequencies precede lower (see the single-pulse theory in Fig. 4). For low field strengths [in the

absence of adiabatic following effects [10,11]] and large negative chirps, this can be understood conceptually as the front of the pulse is only resonant with the $5P$ to $5D$ transition. Since there is no initial population in $5P$ and a resonantly enhanced two-photon transition cannot occur, the only contribution is from the frequencies corresponding to approximately half the $5S$-$5D$ energy splitting. Similar to previous experiments with single-pulse excitation we observe a characteristic oscillation of $5D$ population versus chirp with a period given by $\phi''_{2\pi} = 2\pi/\delta^2$ [13]; the definition of δ is given in Fig. 1(a). The measured period of $\phi''_{2\pi} = 14.5 \times 10^4$ fs^2 agrees well with the theory value of $\phi''_{2\pi} = 14.3 \times 10^4$ fs^2 for $5P_{3/2}$ $F = 3$. However, for negative chirps significantly different results
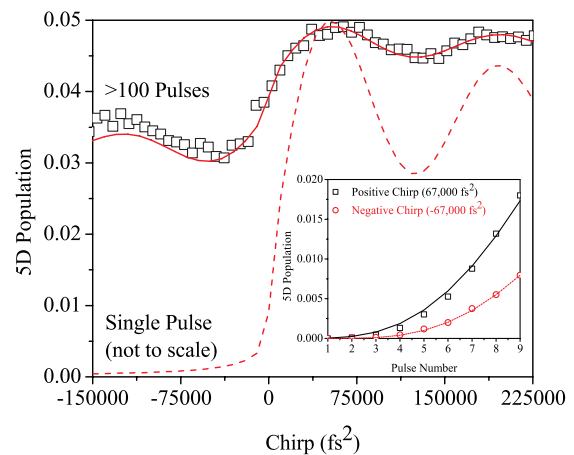

FIG. 4 (color online).   The $5D_{5/2}$ $F = 4$ excited state fluorescence is measured (squares) under steady-state excitation (>100 pulses) vs the applied linear frequency chirp. The solid line indicates the steady-state theory and the dashed line is the single-pulse theory. Inset: the signal (symbols) vs pulse number for two values of equal and opposite chirp; the solid and dashed lines are theoretical predictions.
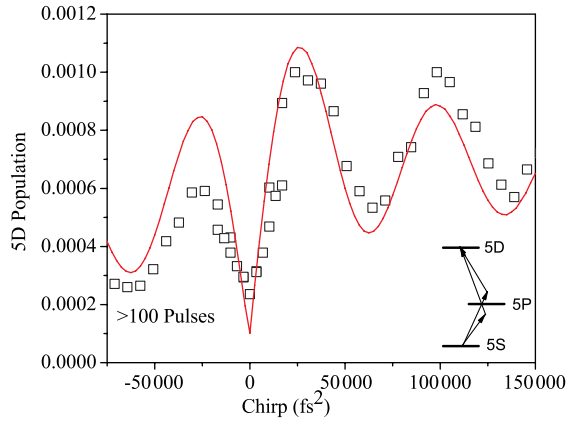
FIG. 5 (color online). Measured fluorescence (squares) and theoretical prediction (solid line) for the case of destructive quantum interference vs linear frequency chirp. The inset shows two of the many two-photon resonant comb mode pairs symmetrically detuned from the intermediate $5P_{3/2}$ $F = 3$ resonance; the closest pair is ± 50 MHz ($\pm f_r/2$) detuned.

are observed for multipulse excitation, as shown in Fig. 4. This difference is due to the 5S-5P electronic coherence that persists for approximately 50 ns, or about five inter-pulse periods. For negative-chirp pulses the intermediate state can be excited by the low-frequency end of the preceding pulse and the high-frequency beginning of the next pulse can complete the two-photon transition. Figure 4 inset shows the 5D population at $\phi'' = \pm 6.7 \times 10^4$ fs^2 versus the number of pulses to illustrate that the scaling of 5D population is smaller for negative chirp. We emphasize that unlike single-pulse experiments our results involve only three well-resolved hyperfine levels chosen such that hyperfine selection rules prohibit any transitions from other states to $5D_{5/2}$ $F = 4$. It is for this reason that we can attribute the measured oscillation period, $\phi''_{2\pi}$, to only one intermediate state. This contrasts previous work where, for example, the $5P_{1/2}$ states exhibit a shorter period, $\phi''_{2\pi} = 2.38 \times 10^3$ fs^2, oscillation superposed on the larger $5P_{3/2}$ signal [13,14].

Our final experiment further demonstrates the versatility of the high resolution frequency comb with spectral phase control by significantly reducing the nonlinear absorption. The phase of the two-photon transition amplitude for a pair of modes is a function of the intermediate state detuning [19]. The detuning of the closest mode to the intermediate $5P_{3/2}$ $F = 3$ state can be tuned from 0 MHz to at most $f_r/2$. In the case of all modes symmetrically detuned around $5P_{3/2}$ $F = 3$, the relative phase between the ± 50 MHz detuned two-photon transition amplitudes is $2 \times \tan^{-1}[2 \times (50 \text{ MHz}/6 \text{ MHz})] \simeq 173°$; between all other further detuned mode pairs it is $\simeq 180°$. This phase flip around the intermediate state results in nearly complete destructive quantum interference of the two-photon transition probability for transform-limited pulses [12].

Translating the entire comb by varying f_o can easily position all mode pairs symmetrically around the intermediate state, while maintaining two-photon resonance (Fig. 5, inset). As shown in Fig. 5, this results in approximately 50 times less 5D population than the previous case when a mode is tuned on $5P_{3/2}$ $F = 3$ resonance. Linear frequency chirp introduces extra relative phase between amplitudes detuned above and below the 5P resonance and reduces the net destructive interference. As shown in Fig. 5, the two-photon transition probability is modulated versus chirp, with a minimum 5D population at zero chirp.

In conclusion, we have demonstrated transient coherent accumulation via a controlled number of phase-coherent femtosecond pulses in an atomic system. The application of spectral phase manipulation to this multipulse regime enables fundamental coherent control experiments to be performed at a resolution limited only by natural resonance widths. The present work is a step towards combining pulse shaping from the field of coherent control with femtosecond comb technology. This research is expected to enable high resolution coherent control, for example, in wave packet shaping for molecular photoassociation [20].

*Permanent address: Instituto de Fisica Gleb Wataghin, UNICAMP, Campinas, SP, 13083-970, Brazil.
†Present address: Fritz-Haber-Institut der Max-Planck-Gesellschaft, D-14195 Berlin, Germany.
[1] Th. Udem, R. Holzwarth, and T. W. Hänsch, Nature (London) **416**, 233 (2002).
[2] S. T. Cundiff and J. Ye, Rev. Mod. Phys. **75**, 325 (2003).
[3] A. Marian et al., Science **306**, 2063 (2004).
[4] A. Marian et al., Phys. Rev. Lett. **95**, 023001 (2005).
[5] S. A. Diddams et al., Science **293**, 825 (2001).
[6] J. Ye, L.-S. Ma, and J. L. Hall, Phys. Rev. Lett. **87**, 270801 (2001).
[7] K. W. Holman et al., Opt. Lett. **30**, 1225 (2005).
[8] R. J. Jones et al., Phys. Rev. Lett. **94**, 193201 (2005).
[9] C. Gohle et al., Nature (London) **436**, 234 (2005).
[10] J. R. Kuklinski et al., Phys. Rev. A **40**, 6741 (1989).
[11] B. Broers, H. B. van Linden van den Heuvell, and L. D. Noordam, Phys. Rev. Lett. **69**, 2062 (1992).
[12] D. Meshulach and Y. Silberberg, Nature (London) **396**, 239 (1998).
[13] P. Balling, D. J. Maas, and L. D. Noordam, Phys. Rev. A **50**, 4276 (1994).
[14] B. Chatel et al., Phys. Rev. A **68**, 041402 (2003).
[15] D. Oron et al., Phys. Rev. Lett. **88**, 063004 (2002).
[16] W. Salzmann et al., Phys. Rev. A **73**, 023414 (2006).
[17] D. Felinto, L. H. Acioli, and S. S. Vianna, Phys. Rev. A **70**, 043403 (2004).
[18] O. E. Martinez, IEEE J. Quantum Electron. **23**, 59 (1987).
[19] T. H. Yoon et al., Phys. Rev. A **63**, 011402 (2001).
[20] J. Vala et al., Phys. Rev. A **63**, 013412 (2001).